

E7-2011-1

S. A. Karamian, J. J. Carroll*, N. V. Aksenov, Y. A. Albin,
G. A. Bozhikov, S. N. Dmitriev, G. Y. Starodub, G. K. Vostokin

PRODUCTION OF ISOMERS IN COMPOUND
AND TRANSFER REACTIONS WITH ^4He IONS

Submitted to «Nuclear Instruments and Methods, A»

*Youngstown State University, Youngstown, Ohio, USA

Карамян С. А. и др.

E7-2011-1

Получение изомеров в реакциях образования составного ядра
и в реакциях передачи нуклонов с ионами ^4He

Хорошо известный остров ядерной изомерии около $A = 175\text{--}180$ обязан своим появлением выстроенности одночастичного углового момента нуклонов вдоль оси деформации при высоких спинах. В некоторых случаях это приводит к образованию многочастичных состояний с рекордным спином, долгоживущих благодаря « K -запрету», т. е. перестройке симметрии. Методы получения и спектроскопические исследования таких изомеров остаются актуальными среди задач современной физики ядерных реакций и изучения структуры ядра. В данной работе радиоактивные продукты получены при облучении мишеней из обогащенного ^{176}Yb (97,6%) и естественного Lu ионами ^4He с энергией 35 МэВ на внутреннем пучке циклотрона U200. Наведенные активности проанализированы с применением методов радиохимии и гамма-спектроскопии. Измерены выходы реакций образования составного ядра и реакций передачи нуклонов, и определены изомерные отношения. Для реакций типа (α, xn) применена стандартная процедура расчета сечений, в то время как для реакций передачи установлена регулярная систематическая зависимость. При описании экспериментальных результатов, в частности изомерных отношений в прямых реакциях с ионами ^4He , получены новые данные о механизме реакций.

Работа выполнена в Лаборатории ядерных реакций им. Г. Н. Флерова ОИЯИ.

Препринт Объединенного института ядерных исследований. Дубна, 2011

Karamian S. A. et al.

E7-2011-1

Production of Isomers in Compound and Transfer Reactions with ^4He Ions

A well-known island of nuclear isomerism appears near $A = 175\text{--}180$ due to the deformation alignment of single-particle orbits at high angular momentum. This sometimes results in the formation of multi-quasiparticle states with record spin that are long-lived because of « K -hindrance», i.e., symmetry rearrangement. Production methods and spectroscopic studies of these isomers remain a challenge for modern nuclear reaction and nuclear structure physics. In the present work, activities were produced by irradiation of ^{176}Yb (97.6%) enriched and $^{\text{nat}}\text{Lu}$ targets with 35-MeV ^4He ions from the internal beam of the U200 cyclotron. Induced activities were analyzed applying methods of radiochemistry and gamma spectroscopy. Yields of compound and nucleon-transfer reactions were measured and the isomer-to-ground state ratios were deduced. Calculated results were obtained using standard procedures to reproduce the (α, xn) cross sections, and the systematic behavior of the nucleon-transfer yields was established. The isomer-to-ground state ratios for direct reactions with ^4He ions were examined, resulting in a new characterization of the reaction mechanism.

The investigation has been performed at the Flerov Laboratory of Nuclear Reactions, JINR.

Preprint of the Joint Institute for Nuclear Research. Dubna, 2011

INTRODUCTION

Standard neutron irradiations in reactors are not sufficiently productive for some radionuclides with special properties, so that it is necessary to use beams of charged particles accelerated in cyclotrons or in larger-scale facilities. High-spin isomers are among such nuclides, because thermal neutrons cannot transfer high angular momentum to the reaction products. Perhaps the most extreme example would be in the accumulation of the four-quasiparticle $16^+ \text{}^{178m2}\text{Hf}$ isomer, which is relevant for exploration of exotic nuclear structure and in a view of possible applications [1]. This interest is derived from the high excitation energy of the isomeric state, 2.446 MeV, giving a large specific energy density near 1.3 GJ/g. The production of $^{178m2}\text{Hf}$ at Los Alamos Laboratory via spallation of Ta by 800-MeV protons was described in [2–4]. There, the beam power could be as high as 1 MW, but by chance this method appeared as a relatively inexpensive production mechanism since massive Ta samples were used as beam dumps in the LAMPF accelerator. The isomer was accumulated as a by-product of unrelated experiments and with a relatively high absolute yield. However, the great level of total activity, due to the presence of many radioactive impurities in the Hf fraction even past chemical isolation, makes this method disadvantageous for use in some experiments and applications.

The spallation method for isomer production was studied in more detail in a series of experiments with the Dubna synchrocyclotron [5–7]. Targets of $^{\text{nat}}\text{Re}$, $^{\text{nat}}\text{W}$, ^{186}W , $^{\text{nat}}\text{Ta}$, $^{\text{nat}}\text{Hf}$ and ^{179}Hf were irradiated with protons at energies varying from 100 to 650 MeV. The conclusion was reached that production of $^{178m2}\text{Hf}$ would be more economic with irradiations by 100 MeV protons at some medium-class cyclotron facility as compared to 800-MeV protons at a facility like LAMPF/LANSCE. The lower energy protons allow a less massive target and, therefore, a much-reduced total activity of the material that must then be processed chemically. There would also be a reduced yield of nuclides, both active and stable, which would act as background to extraction of a specific radioisotope of interest. These effects were confirmed for the high-spin isomers ^{177m}Lu , $^{178m2}\text{Hf}$, and $^{179m2}\text{Hf}$ [5–7]. In those works, the isomer-to-ground state ratios were deduced and analyzed to clarify the reaction mechanism.

Another method for production of high-spin isomers was proposed earlier, studied and developed within the European collaboration exploiting the neutron evaporation reaction $^{176}\text{Yb}(\alpha, xn)$ with a ^4He ion beam [8, 9]. The absolute productivity was lower as compared to the spallation reaction, but the presence of fewer reaction products meant that a more «pure» material was created for accumulation of a specific species of interest. As much as of about $1\ \mu\text{g}$ of $^{178m2}\text{Hf}$ was accumulated after extensive irradiations with the Dubna U200 cyclotron. It was then possible to arrange in Orsay a mass separation of Hf, isolating $^{178m2,g}\text{Hf}$ from other long-lived and stable isotopes [8, 10]. A series of nuclear spectroscopic experiments were performed using the $^{178m2}\text{Hf}$ target and the results were reviewed in [9, 11].

The present work was performed to develop systematic measurements of the yields for all activities, including isomers, produced in $^4\text{He} + ^{176}\text{Yb}$ and $^4\text{He} + \text{natLu}$ irradiations. The absolute yields, σ_m/σ_g ratios and features of the reaction mechanisms were of interest in the course of this experimental study and the corresponding theoretical analyses. The observed nuclear reactions could be split on two classes: fusion-evaporation past compound nucleus formation, and nucleon-transfer (direct) reactions. The behavior of the cross sections is very different for these two classes of reactions.

1. EXPERIMENTS

Targets were composed of 97.6% enriched ^{176}Yb and natural Lu materials in the form of oxides, and were irradiated by the internal beam of the U200 cyclotron at JINR, Dubna. The isotopic composition of the enriched Yb target is given in Table 1. The natural Lu material contained 97.4% of ^{175}Lu and 2.6% of ^{176}Lu . Despite its low content, the latter isotope could play a significant role since it possesses the anomalously high ground-state spin of 7 essential for population of isomers in reaction products.

Table 1. Isotope composition of the enriched ^{176}Yb material

Mass number	171	172	173	174	176
Content, %	0.07	0.22	0.18	1.93	97.6

An aluminum target holder with internal water flow provided effective cooling of the target layer. The thickness of Al between the Yb or Lu oxide layer and the water was only 1.5 mm for the best heat removal. Reactor grade (high purity) Al was used for construction of the holder to insure the minimum production of additional activities that would serve as impurities, and for the best possible thermal conductivity. Target layers of Yb_2O_3 and Lu_2O_3 were prepared on the polished and cleaned Al substrate by spreading a nitrate solution of Yb or Lu

in alcohol over the surface, followed by drying and heating to cause conversion of the nitrate to oxide. The process was repeated, so that the total layer finally reached a thickness of 7.5 mg/cm^2 in the metal content.

The holder with the target layer was inserted into the cyclotron chamber at the final radius of acceleration and was aligned at 5 degrees with-respect-to the internal beam direction. With this small inclination angle, the effective thickness of the layer was increased and the beam power was distributed over a large area of 12 cm^2 for maximum heat removal. The $^4\text{He}^+$ ion energy at the extraction radius was $(35 \pm 0.5) \text{ MeV}$ and corresponded to a beam power of about 500 W at a beam current restricted to be $\leq 15 \text{ }\mu\text{A}$. The sample construction could withstand $3\times$ higher beam power, but the current was restricted due to radiation safety conditions owing to the intense neutron flux generated by the target under the beam.

The effective target layer thickness of 86 mg/cm^2 (of the metal) projected to the beam direction leads to about 10 MeV energy loss for the ^4He ions, accounting for stopping in the target oxide material. Therefore, the irradiation conditions corresponded to a beam energy between 35 and 25 MeV. The semi-thick target increased the absolute yield of reactions, but in some cases deteriorated the isomer-to-ground state ratio due to the changed beam energy range.

After irradiation, the target material was washed off the backing with 16 M HNO_3 . Naturally, some small part of the Al substrate was also removed and included in the chemical processing. Carbon was also present in the removed material, since carbon deposits onto any target under irradiation in a cyclotron because of traces of oil vapor in the vacuum. The carbon was removed by filtration prior to further chemical processing of the solution. Gamma-activity measurements confirmed that no significant amount of the reaction products of interest herein had been collected in the carbon material. An anion exchange in a concentrated HCl solution was applied to separate the Hf fraction. Precipitations of YbF_3 and LuF_3 were also performed. Deep purification of the materials was carried out using anion and cation exchange chromatography with an overall chemical yield higher than 80%. The purity of the separated products was controlled by gamma spectroscopy.

Gamma spectra were measured with an HPGe detector for the materials prior to chemical processing and for the isolated elemental fractions. For some sources, the measurements were carried out many times past the irradiation during a long calendar time on the scale of half a year. The energy resolution of the detector was better than 1.8 keV for the ^{60}Co γ lines and the detector-source distance was varied to keep the dead time lower than 20% to avoid degradation of the spectral resolution. A commercial set of standard radioisotope sources was used for absolute efficiency calibration of the detector. The number of atoms of a given reaction product was then determined by applying the well-known equations for time and efficiency factors accounting for accumulation and decay.

The absolute quantum yields for γ lines were taken from the Nuclear Data Sheets [12]. Finally, the accuracy for many of the measured yields reached about 10%, including errors in literature quantum yields, detector efficiency, etc. For some product activities, the accuracy was reduced by the presence of only low-intensity γ lines. For processing and decomposition of the complex γ spectra, the «Genie 2000» program was used, from which the γ -line energy, peak area and statistical error were obtained. A tentative attribution was also possible using a standard database, but was not used because that function could be more reliably defined from the known set of possible reactions.

Lists of the radioactive nuclides obtained from the irradiated targets of ^{176}Yb and $^{\text{nat}}\text{Lu}$ are given in Tables 2 and 3, respectively. The nuclide half-life, producing reaction, the reaction threshold and relative yield measured by gamma spectroscopy are given in those tables. Reactions with emission of several nucleons can be written in the form of the composite ejectile emission: for instance, writing $(\alpha, {}^2\text{H})$ instead of (α, pn) . Both designations correspond to the creation of identical reaction products and reactions like $(\alpha, {}^2\text{H})$ and (α, pn) could not be differentiated in the present data. However, emission of a deuteron is characterized by a lower reaction threshold than emission of the pn combination of ejectiles, and similarly for a triton compared with the $p2n$ combination. The reaction with lower threshold should be preferred, since it would correspond to a higher cross section at a given energy. Thus, the designation $(\alpha, {}^2\text{H})$, etc. is used in Tables 2 and 3. Also, different thresholds exist for reactions depending on whether the product is in an isomeric or ground state, and both are given in the tables.

The minor isotopes in the enriched ^{176}Yb target, namely $^{171-174}\text{Yb}$, still generated observed activities. For instance, the products of $^{171-173,175}\text{Hf}$ were manifested very well in the gamma spectra. In some cases, the same product may result from different reactions with different target Yb isotopes and Table 2 contains all relevant thresholds. The Lu target contains only two isotopes and the corresponding reactions are written on separate lines in Table 3. The relative measured reaction yields in the tables were normalized to the calculated yield of the most probable fusion evaporation reactions. In the 35–25 MeV ${}^4\text{He}^+$ beam range, the largest cross sections should correspond to $(\alpha, 2n)$ reactions. The most abundant isotopes in the targets were ^{176}Yb and ^{175}Lu . Thus, the reactions $^{176}\text{Yb}(\alpha, 2n)^{178m2,g}\text{Hf}$ and $^{175}\text{Lu}(\alpha, 2n)^{177}\text{Ta}$ were selected to normalize the Yb and Lu reaction yields, respectively.

From the Yb irradiation, the total yield of ^{178}Hf could not be measured directly because the ground state is stable and produces no delayed γ -radiation signal: only the yield of the $^{178m2}\text{Hf}$ isomer was determined by its gamma activity. However, an absolute calibration could be performed by exploiting the measured yield of ^{175}Hf from reactions on $^{173,174}\text{Yb}$. The latter yield as well as the yield for $^{178m2}\text{Hf} + ^{178g}\text{Hf}$ were calculated, using the method described in the

Table 2. List of produced radionuclides and corresponding reactions observed with the enriched ^{176}Yb (97.6%) target

Product	Half-life	Reaction	Threshold, E_{th} , MeV	Rel. yield*	
				Exp. (err., %)	Calc.
^{175}Yb	4.2 d	$^{176}\text{Yb}(\alpha, \alpha' n)$	6.86	$4.4 \cdot 10^{-2}$ (8)	—
^{171}Lu	8.22 d	daughter of ^{171}Hf	—	$4.8 \cdot 10^{-5}$ (14)	$7.5 \cdot 10^{-5}$
^{172}Lu	6.7 d	daughter of ^{172}Hf	—	$6.31 \cdot 10^{-4}$ (7)	$1.0 \cdot 10^{-3}$
^{173}Lu	1.37 y	daughter of ^{173}Hf	—	$2.74 \cdot 10^{-3}$ (7)	$3.32 \cdot 10^{-3}$
^{174g}Lu	3.31 y	$^{172}\text{Yb}(\alpha, ^2\text{H})$ $^{173}\text{Yb}(\alpha, ^3\text{H})$	14.40 14.51	$2.6 \cdot 10^{-5}$ (9)	—
^{174m}Lu	142 d	$^{172}\text{Yb}(\alpha, ^2\text{H})$ $^{173}\text{Yb}(\alpha, ^3\text{H})$	14.57 14.68	$1.0 \cdot 10^{-5}$ (11)	—
^{177g}Lu	6.65 d	$^{176}\text{Yb}(\alpha, ^3\text{H})$	13.64	$6.6 \cdot 10^{-3}$ (12)	—
^{177m}Lu	160.5 d	$^{176}\text{Yb}(\alpha, ^3\text{H})$	14.61	$2.6 \cdot 10^{-4}$ (18)	—
^{171}Hf	12.2 h	$^{171}\text{Yb}(\alpha, 4n)$	33.7	$4.8 \cdot 10^{-5}$ (14)	$7.5 \cdot 10^{-5}$
^{172}Hf	1.87 y	$^{(168+x)}\text{Yb}(\alpha, xn)$, $x = 3-4$	24.7; 32.7	$6.31 \cdot 10^{-4}$ (7)	$1.0 \cdot 10^{-3}$
^{173}Hf	23.6 h	$^{(169+x)}\text{Yb}(\alpha, xn)$, $x = 2-4$	17.6; 25.6; 32.0	$2.74 \cdot 10^{-3}$ (7)	$3.32 \cdot 10^{-3}$
^{175}Hf	70 d	$^{(171+x)}\text{Yb}(\alpha, xn)$, $x = 2-3$	16.8; 24.3	0.024 (5.1)	0.024
$^{178m2}\text{Hf}$	31 y	$^{176}\text{Yb}(\alpha, 2n)$	17.22	0.023 (6)	1.00**
$^{179m2}\text{Hf}$	25.1 d	$^{176}\text{Yb}(\alpha, n)$	9.78	$1.5 \cdot 10^{-3}$ (5.3)	$1.2 \cdot 10^{-2}$ **

* Normalized to the calculated yield of the $^{176}\text{Yb}(\alpha, 2n)$ reaction as described in the text.

** Corresponds to the total yield of ^{178}Hf or ^{179}Hf .

next section. If the ^{178}Hf yield is taken as unity, then the ^{175}Hf yield will have a relative value of 0.024. Finally, the experimental yield of ^{175}Hf was given in relative scale as 0.024, so that it and other yields in Table 2 were normalized relative to ^{178}Hf . Experimental yields for definite isotope products were obtained from gamma spectroscopy and many of them were small due to the low abundance of the target isotope responsible for the particular reaction. Thus, the yields in Tables 2 and 3 are not yet the physical yields of the reactions. For comparison and simulations, they must be scaled to 100% content in a hypothetical target.

In practice, it is important to characterize the absolute yield of the $^{178m2}\text{Hf}$ isomer. In the present ^{176}Yb target configuration, the measured yield was about 3 isomeric nuclei per 10^6 ^4He beam ions. With the $^4\text{He}^+$ ion beam current of $15\ \mu\text{A}$, the yield corresponds to the production of a total of $2.5 \cdot 10^{13}$ atoms of $^{178m2}\text{Hf}$ per day of the irradiation. The absolute yields of other reaction products can be found using the information in Table 2.

From the Lu irradiation, the total yield of ^{177}Ta included a contribution from the $^{176}\text{Lu}(\alpha, 3n)$ reaction. Thus in Table 3, the normalization of the Lu sample reaction products was taken to the total yield of ^{177}Ta by $^{175}\text{Lu}(\alpha, 2n)$ and $^{176}\text{Lu}(\alpha, 3n)$ reactions. It is important to note that calculated yields only appear in Tables 2 and 3 for those reactions designated by «compound», as described below.

2. DATA ANALYSIS AND SIMULATION

Among the entries in Tables 2 and 3, two different classes of reactions may be distinguished, namely: fusion-evaporation («compound») and transfer («direct») reactions. More exactly, the terms of transfer and direct reactions are not absolutely identical as they stress slightly different reaction properties. For instance, the $(\alpha, ^3\text{He})$ reaction definitely corresponds to the transfer of one neutron from the projectile to the target, while $(\alpha, \alpha'xn)$ happens in direct reactions by neutron knock-out or by deep inelastic α scattering with strong excitation of the residual nucleus. Then neutrons are emitted because emission of the weekly-bound $^{(4+x)}\text{He}$ isotopes is improbable. Nevertheless, in this work transfer and true direct reactions will not be differentiated as the reactions herein designated as «direct» all include emission of charged ejectiles in the exit channel. Clearly, neutron evaporation from a compound nucleus (c.n.) is in another reaction class, proceeding via another mechanism.

For compound reactions, the simulation of neutron evaporation is a common problem resolved within the statistical model. Specific algorithms were developed and accepted more than fifty years ago, based on the idea that the xn evaporation cross section may be expressed as the product of two functions: the cross section $\sigma_c(E)$ for formation of the compound nucleus, and the probability of emission

$P_x(E)$ of x neutrons. Both factors are taken to be functions of the c.n. excitation energy E , the thermal excitation U or the incoming projectile energy. Such a general scheme originated in the 1960s (see, for instance, [13]) and statistical P_x functions were developed by Jackson [14].

To describe (α, xn) reactions in the present work, a standard procedure in the style of the Jackson–Sikkeland approach [13, 14] was used. The $P_x(E)$ equations in the most accurate mathematical form were taken from [15]. The most important parameter of the nuclear temperature T was calculated using the Fermi-gas model with level-density parameter $a = A/8$. The cross section for c.n. formation was determined with Coulomb barrier of interaction energy B_c using the Bass equation [16], the most popular choice in the literature in recent decades. The magnitude of B_c defines the position and slope of the $\sigma_c(E)$ function, while the nuclear size parameter r_0 is responsible for the absolute cross sections and does not influence their ratios. Because relative yields were measured and analyzed herein, making a perfect choice for r_0 is, therefore, not critical.

The calculated excitation functions are shown in Figs. 1 and 2 for the $^{176}\text{Yb}(\alpha, xn)$ and $^{175}\text{Lu}(\alpha, xn)$ reactions, respectively. For other target isotopes of $^{171-174}\text{Yb}$ and ^{176}Lu similar functions were calculated. Emission of pre-equilibrium neutrons is not very probable at $E_\alpha \leq 35$ MeV and so only slightly influences the shown excitation functions. The exception is the (α, n) reaction,

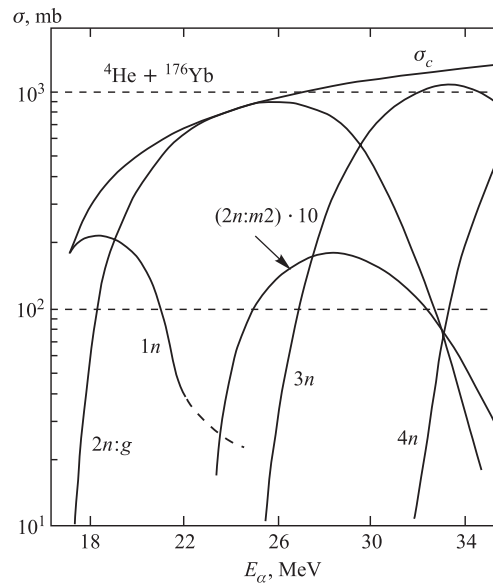


Fig. 1. Excitation functions of $^{176}\text{Yb}(\alpha, xn)$ reactions calculated using a Fermi-gas model within the formalism of Jackson–Sikkeland [13, 14], and using formulae of [15] for the best correctness

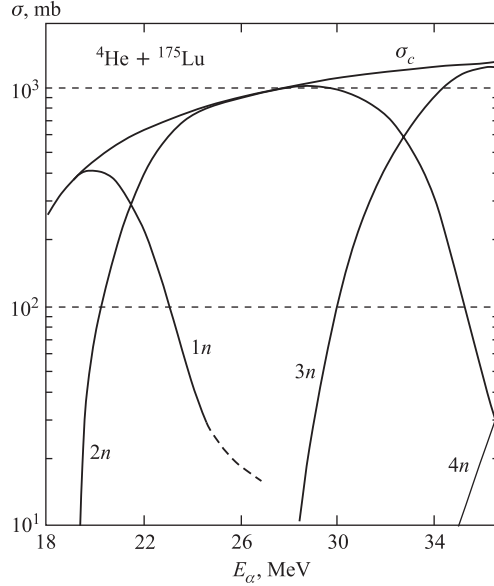


Fig. 2. The same as in Fig. 1, but for $^{175}\text{Lu}(\alpha, xn)$ reactions

where the excitation function demonstrates a tail to higher energies, as shown in the figures. The high-spin $^{178m2}\text{Hf}$ isomer could be populated when the $(\alpha, 2n)$ reaction residue possesses a spin higher than 16. However, in reactions producing a compound nucleus such values of angular momentum appear with reduced probability at energies near and below the maximum of the $(\alpha, 2n)$ excitation function. Thus, the excitation function for $^{178m2}\text{Hf}$ is shifted by 5 MeV to higher energy in Fig. 1, relative to the excitation function for ^{178g}Hf , although its right slope remains practically at the same position as for the $(\alpha, 2n)$ reaction in total, because of strong competition from the $3n$ evaporation channel. Finally, the $^{178m2}\text{Hf}$ -producing excitation function shown in Fig. 1 has a much lower width than the other functions in that figure. In ordinate, the maximum value of the excitation function is defined via the $^{178m2}\text{Hf}/^{175}\text{Hf}$ yield ratio in combination with the reliably-calculated yield for the $^{174}\text{Yb}(\alpha, 3n)^{175}\text{Hf}$ reaction. For both $^{178m2}\text{Hf}$ and $^{179m2}\text{Hf}$ isomers, the yields were measured and shown in Table 2 although the corresponding ground-states yields could not be directly measured. Still, the calculated total yields of ^{178}Hf and ^{179}Hf using the corresponding $2n$ and $1n$ excitation functions in Fig. 1 allow an estimate of the σ_m/σ_g ratios.

The reaction yield was successfully calculated by integration of the excitation functions over the energy range from 25 to 35 MeV, defined by stopping of the projectile ions in the semi-thick target. The stopping power function entered as

Table 3. List of the produced radionuclides and corresponding reactions observed with the ^{nat}Lu target

Product	Half-life	Reaction	Threshold, E_{th} , MeV	Rel. yield*	
				Exp. (err., %)	Calc.
^{175}Yb	4.2 d	$^{175}\text{Lu}(\alpha, ^3\text{He } p)$ $^{176}\text{Lu}(\alpha, \alpha' p)$	20.27 5.98	$0.83 \cdot 10^{-4}$ (33)	–
^{172}Lu	6.7 d	$^{175}\text{Lu}(\alpha, \alpha' ^3m)$	22.64	$1.27 \cdot 10^{-5}$ (30)	–
^{173}Lu	1.37 d	$^{175}\text{Lu}(\alpha, ^6\text{He})$	13.45	$1.47 \cdot 10^{-3}$ (9)	–
^{174g}Lu	3.31 y	$^{175}\text{Lu}(\alpha, \alpha' n)$	7.67	$2.76 \cdot 10^{-2}$ (7)	–
^{174m}Lu	142 d	$^{175}\text{Lu}(\alpha, \alpha' n)$ $^{176}\text{Lu}(\alpha, ^6\text{He})$	7.84 13.15	$1.18 \cdot 10^{-2}$ (8)	–
^{177g}Lu	6.65 d	$^{175}\text{Lu}(\alpha, 2p)$	14.94	$2.8 \cdot 10^{-4}$ (17)	–
^{177m}Lu	160.5 d	$^{175}\text{Lu}(\alpha, 2p)$ $^{176}\text{Lu}(\alpha, ^3\text{He})$	15.91 14.47	$1.7 \cdot 10^{-5}$ (13)	–
^{175}Hf	70 d	daughter of ^{175}Ta	–	$0.97 \cdot 10^{-3}$ (6)	$0.5 \cdot 10^{-3}$
$^{178m2}\text{Hf}$	31 y	$^{175}\text{Lu}(\alpha, p)$ $^{176}\text{Lu}(\alpha, ^2\text{H})$	10.04 14.10	$2.6 \cdot 10^{-3}$ (15)	–
$^{179m2}\text{Hf}$	25.1 d	$^{176}\text{Lu}(\alpha, p)$	8.89	$2.4 \cdot 10^{-4}$ (7)	–
^{175}Ta	10.5 h	$^{175}\text{Lu}(\alpha, 4n)$	32.63	$0.97 \cdot 10^{-3}$ (6)	$0.5 \cdot 10^{-3}$
^{176}Ta	8.08 h	$^{175}\text{Lu}(\alpha, 3n)$	25.59	0.49 (9)	0.47
^{177}Ta	2.36 d	$^{175}\text{Lu}(\alpha, 2n)$; $^{176}\text{Lu}(\alpha, 3m)$	17.17; 23.46	1.0 (5.3)	1.0

*Normalized to the calculated yield of the $^{175}\text{Lu}(\alpha, 2n)$ + $^{176}\text{Lu}(\alpha, 3m)$ reactions as described in the text.

the inverse, $(dE/dx)^{-1}$, to provide the integration of the reaction yield over the target thickness. The calculated yields determined in this way for compound-nucleus reactions are those displayed, with the previously described normalization, in Tables 2 and 3. Direct reaction yields could not be calculated with this procedure, but the evaporation product yields were satisfactorily reproduced. Even yields at a relative level of 10^{-4} – 10^{-5} in Tables 2 and 3 deviate between the calculated and measured by a factor not higher than 1.5. The agreement of calculated and measured yields across such a wide range of magnitudes confirms the calculations both in general approach and in the choice of specific numerical parameters. It should be noted that the lowest yields in Table 2 correspond to reactions with low-abundant target isotopes present in the enriched ^{176}Yb target, as given in Table 1 from the original material assay. Possible inaccuracies in those values could be responsible for the mentioned maximum deviation factor of 1.5 between calculated and measured yields. The $^{178m2}\text{Hf}$ and $^{179m2}\text{Hf}$ isomers are formed with the target isotopes of larger (and thus, better-known) content, and the calculated yields could be relied upon to estimate of the σ_m/σ_g ratios.

In Table 3, only three evaporation reactions provide a comparison of experimental and calculated yields. The agreement is satisfactory, in general, although the calculations for the $(\alpha, 4n)$ reaction show some deviation from the measured yield. This may be explained by the sensitivity of this reaction yield to the projectile energy, since the excitation function has a sharp cut-off near the initial beam energy of 35 MeV. The other reactions with the $^{\text{nat}}\text{Lu}$ target are of the direct type and another approach is needed. Calculations are impossible for many reactions listed in Tables 2 and 3. For cross sections of direct reactions with heavy ions, the Q -ground-ground (Q_{gg}) systematic behavior has been known for many decades [17], but that was not well demonstrated for α -induced reactions. In the present studies, the yield of isomers is of primary interest and the Q_{gg} parameter is not applicable to such excited rather than ground states. The reaction threshold can be used as a parameter, but, in principle, it is better to parameterize the yields by the excess projectile energy in the center-of-mass (c.m.) system above the reaction threshold, which makes the real influence. For direct reactions, the excess projectile energy supplies more phase volume in momentum space for emission of charged particles and the cross section is correspondingly increased.

In Fig. 3, the reaction yields are plotted as a function of $(E_c - E_{\text{th}})$, where the c.m. kinetic energy of the ^4He beams ions, E_c , is taken to be 32 MeV, based on the incident beam energy. The E_{th} is the reaction threshold energy. It can be assumed that direct reactions are characterized by strongly growing excitation functions and so E_c should be used at a value greater than the simple mean energy over the target thickness. A more exact value of E_c would be the weighted mean of the ion energy over the target thickness. Nevertheless, a more or less arbitrary choice of E_c has little real effect on the systematics seen in Fig. 3, since variation in E_c leads only to translation (parallel shift) of the dependence.

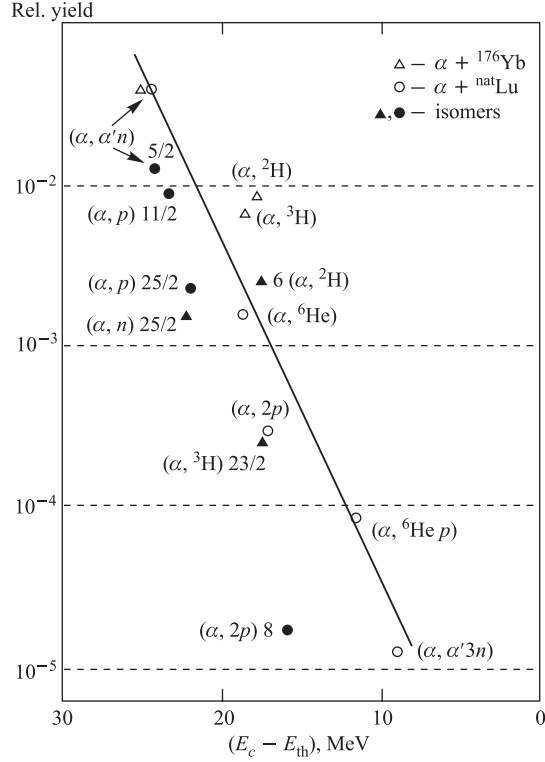


Fig. 3. Direct reaction yields measured in the present studies and systematized over the parameter characterizing the excess energy above the reaction threshold. Points correspond to the total and isomeric yields obtained in reactions with both ^{176}Yb and $^{\text{nat}}\text{Lu}$ targets

The major influence is due to the threshold parameter, which is unique to each specific reaction. Its numerical values are given in Tables 2 and 3 according to the standard nuclear mass data.

The yields in those tables are proportional to the abundance of the target isotope responsible for the production of a specific product. Thus, the observed yields of some products are due to low-abundance isotopes. To establish a physical comparison, it was necessary to correct the measured yields from the true abundances to a hypothetical abundance of 100% for all reactions. Therefore, the physical reaction yields are shown in Fig. 3 instead of the measured radionuclide yields.

The total ($m + g$) yields are shown in Fig. 3 by the open points and the isomeric yields by filled points. The spin-difference parameter $I_m - I_t$, where I_m is the isomer spin and I_t is the target nucleus spin, is given for each plotted point

corresponding to an isomer. It is clear that the filled points are (and must be) located systematically lower than the corresponding open points. In general, Fig. 3 shows an exponential decrease of the total reaction yield with growing threshold, evident despite some scattering of the points. The scattering for transfer reactions is largely due to the secondary process of neutron emission from an excited product. This effect was understood many years ago [18] and has been applied recently [19] in the analysis of nucleon transfer reactions with heavy ions. This process may be illustrated using the following example: Assume that two neutrons are transferred to a heavy target nucleus from a projectile. The nucleus should then have sufficient excitation to evaporate one neutron at a second stage of the reaction. The final product corresponds, therefore, to the cumulative transfer of only one neutron. Such a relaxation process results in an increased yield of the one-neutron transfer product and in a decreased yield of the two-neutron transfer product.

The increased yields of $(\alpha, ^2\text{H})$ and $(\alpha, ^3\text{H})$ reactions seen in Fig. 3 could occur due to similar contributions from higher-probability (α, p) and (α, d) processes, after additional neutron evaporation. Likewise, exotic reactions like $(\alpha, ^6\text{He})$ and $(\alpha, \alpha'3n)$, may have their yields enhanced by more probable $(\alpha, \alpha'n)$ and $(\alpha, \alpha'2n)$ reactions in the same way. In contrast, the $(\alpha, 2p)$ reaction yield is suppressed due to the emission of an additional neutron that would move its product to correspond to the $(\alpha, 2pn)$ channel. Despite these complications, the plot in Fig. 3 may serve as a crude representation of the total reaction yields and for estimates of the σ_m/σ_g ratios. Particularly relevant cases are the $^{178m2}\text{Hf}$ and $^{179m2}\text{Hf}$ isomers, produced in direct reactions with the $^{\text{nat}}\text{Lu}$ target, because their σ_g could only be determined using the systematic trend. For ^{174}Lu and ^{177}Lu product nuclides, both isomer and ground states are radioactive and were, therefore, detectable by γ spectroscopy.

Table 4 lists the deduced isomer-to-ground state ratios from reactions with ^4He ions. This includes the ratios of directly measured isomer yields to ground-state yields, where available, and values deduced from measured isomer yields and calculated (for compound) or estimated (for direct, from Fig. 3) ground-state yields, where necessary. It is clear that the calculations, and especially the estimated total yields, could not be determined with high accuracy and systematical error was included in the uncertainty quoted in Table 4. In some cases, the σ_m/σ_g values could only be deduced with 50% error. These data are nevertheless useful, because no regular survey of isomer-to-ground state ratios has been previously developed for transfer reactions.

Some fragmentary data on isomer-to-ground state ratios are known in the literature [20–23], but correspond only to (α, xn) reactions. The results published in [8, 24, 25] are incorporated with the present results in Table 4. It is clear that in the previous irradiations [8] of the ^{176}Yb target, the isomer-to-ground state ratio was found to be higher for $^{178m2}\text{Hf}$ and lower for $^{179m2}\text{Hf}$ as compared to

Table 4. Isomer-to-ground state ratios obtained in reactions with ^4He ions

Nuclides	Isomer spin	Reaction(s)	Projectile energy, MeV	σ_m/σ_g	Error, %	Ref.
$^{174m,g}\text{Lu}$	6	$^{175}\text{Lu}(\alpha, \alpha' n)$	35*	0.42	15	Present
		$^{172,173}\text{Yb}(\alpha, ^2\text{H}; ^3\text{H})$	35*	0.38	20	Present
$^{177m,g}\text{Lu}$	23/2	$^{176}\text{Yb}(\alpha, ^3\text{H})$	35*	0.04	30	Present
		$^{176}\text{Yb}(\alpha, ^3\text{H})$	36	0.05	30	[24]
		$^{175,176}\text{Lu}(\alpha, 2p; ^3\text{He})$	35*	0.06	30	Present
$^{178m2,g}\text{Hf}$	16	$^{176}\text{Yb}(\alpha, 2n)$	35*	0.024	15	Present
		$^{176}\text{Yb}(\alpha, 2n)$	36	0.05	30	[8]
		$^{175,176}\text{Lu}(\alpha, p; ^2\text{H})$	35*	0.18	50	Present
$^{179m2,g}\text{Hf}$	25/2	$^{176}\text{Lu}(\alpha, p)$	35*	0.35	30	Present
		$^{176}\text{Yb}(\alpha, n)$	35*	0.12	30	Present
		$^{176}\text{Yb}(\alpha, n)$	36	0.07	50	[24]
$^{178m,g}\text{Ta}$	7**	$^{177}\text{Hf}(\alpha, ^3\text{H})$	36	0.3	30	[25]

*Maximum energy with semi-thick target (range of about 10 MeV).

** Isomer assumed to be of high-spin; unambiguous identity of low-energy doublet members with spins of 1 and 7 not yet determined.

the present results. This may be understood as due to the thinner target in the work of [8], resulting in a correspondingly narrower energy range. From the excitation functions shown in Fig. 1, it is evident that the isomer-to-ground state ratios are very sensitive to the chosen energy range of the beam ions, while the absolute isomer yield may be less sensitive to such changes. These predictions are confirmed by comparing the results of the present and previous experiments [8]. The isomer-to-ground state ratio for $^{178m2}\text{Hf}$ should indeed be higher for the beam energy range of 36–30 MeV in [8] as compared to the 35–25 MeV presently used.

For the transfer reactions, it may reasonably be assumed that direct emission of the charged particle will carry away some angular momentum and so the residue has a lower spin than reaction products after c.n. formation. However, it may be argued that transfer reactions take place mostly as peripheral collisions characterized by the maximum impact parameter. In the case of heavy ions, regular studies were published by the Canberra group [26] on the detection of high-spin nuclear levels, excited past incomplete fusion. Significant feeding of high-spin states and isomers was observed with a probability of about 10% at spins near 16. A similar result was obtained in [27] with a target as heavy as ^{238}U exposed to ^{16}O ions. However, for transfer reactions with ^4He ions too few studies have been available from which one could determine regular behavior in their cross sections and in the isomer-to-ground state ratios. Thus, the present results summarized in Table 4 represent a new characterization of the angular momentum released in direct reactions. A plot of the isomer-to-ground state ratios in Table 3 as functions of the spin difference is shown in Fig. 4*.

A large spin difference should suppress the yield of an isomeric state. Such a trend is manifested for both compound and transfer products, as shown in Fig. 4, but the results are clearly grouped according to the two reaction classes. It is possible to distinguish the following regular features: a) fusion-evaporation products are characterized by higher isomer-to-ground state ratios than are nucleon-transfer products; b) at a spin difference approaching zero, the isomer-to-ground state ratio tends to unity for both classes of reactions; and c) at a spin difference near 16, the ratio is decreased to a level of only several percent. The data plotted in Fig. 4 were obtained with the same ^4He projectiles and, therefore, the systematic trend could be seen more clearly than when a comparison is made between reactions in-

*Some plotted points in Fig. 4 do not correspond exactly to entries in Table 3. For example, the yield of $^{174m,g}\text{Lu}$ product radionuclides contains contributions from $^{172}\text{Yb}(\alpha, ^2\text{H})$ and $^{173}\text{Yb}(\alpha, ^3\text{H})$ reactions. Target nuclei of ^{172}Yb and ^{173}Yb have similar (and minor) abundances, as listed in Table 1. The emission probability of tritons is orders-of-magnitude lower than that of deuterons, but the higher target spin of ^{173}Yb ($5/2$) may enhance the isomer-to-ground state ratio for ^{174}Lu . Overall, it was assumed that about 25% of the $^{174m,g}\text{Lu}$ ratio is due to the $^{173}\text{Yb}(\alpha, ^3\text{H})$, so that 75% of the tabulated value of 0.38 was plotted and attributed to the $^{172}\text{Yb}(\alpha, ^2\text{H})$ reaction. A similar approach was followed for the $^{175;176}\text{Lu}(\alpha, 2p; ^3\text{He})$ and $^{175;176}\text{Lu}(\alpha, p; ^2\text{H})$ reactions.

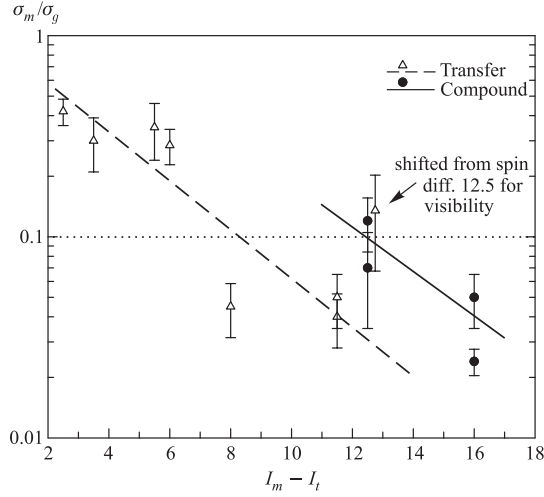


Fig. 4. Experimentally determined isomer-to-ground state ratios as a function of the spin difference parameter ($I_m - I_t$). Compound and transfer reactions are distinguished by the symbols. When both stable isotopes in Lu targets made a contribution to an observed yield, the result was attributed to the main ^{175}Lu target isotope after subtraction of the minor part due to the ^{176}Lu target isotope

duced by different projectiles (see, for instance, [28]). The latter type of analysis requires calculations of the spin distributions created by the different projectiles, generating additional systematical errors and scattering of the results. In [29] data are collected on isomer-to-ground state ratios for Hf isomers produced in reactions with neutrons. A straight-forward unification of those values with the present results may be difficult, but some common behavior could be seen in the style of $\sigma_m/\sigma_g \approx 1$ at low-spin difference.

The behavior described above under a) confirms that the direct reaction ejectile carries away a significant part of the total angular momentum of the α projectile. Thus, for direct reactions the idea that they are peripheral collisions with a tangential impact is obviously not confirmed for the case of moderate-energy ^4He ions. The direct reaction may happen with reasonable probability over a wide range of impact parameters and the transferred spin is systematically reduced as compared to the complete fusion of the projectile and target. The isomer-to-ground state ratio is correspondingly reduced, in agreement with the results displayed in Fig. 4. Such a conclusion seems significant in physical sense. For heavy ions, the mechanism could be different, considering the much shorter wavelength of heavy particles as compared to alphas. The wave packet of alpha particle could spread over the whole range of the available impact parameters.

SUMMARY

The production of isomers and other radioactive products has been studied by the activation method following irradiations of enriched ^{176}Yb and natural Lu targets by ^4He ions. In both cases, at least thirteen radioactive nuclear species were characterized by their measured yields. The relative yields of the compound reactions were calculated theoretically and satisfactory agreement was reached with the measurements. The isomer-to-ground state ratios were determined and discussed for nine reactions including different types, i.e., fusion-evaporation (compound) and the nucleon transfer (direct). The ratio was found to be reduced with an increase in the spin difference between isomer and target, both for direct and compound products. For direct reactions, the total yield decreases with increased reaction threshold. The isomer-to-ground state ratios in direct reactions are systematically lower than those observed for compound-nucleus products. The latter behavior confirms that the charged ejectile carries away a significant part of the total angular momentum, while influence of the expected high impact parameter for direct reactions was not clearly demonstrated. The wave-length of alphas at 7–17 MeV above the Coulomb barrier is not negligible, being of several fm in the present case. Due to that, the differentiation of the reaction type over the impact parameter b is smoothed allowing all reaction mechanisms probable at low and high b values.

Acknowledgements. The authors gratefully acknowledge the U200 cyclotron staff for the beam supply, and S. A. K. and J. J. C. acknowledge support by DTRA through grant HDTRA1-08-1-0014.

REFERENCES

1. Carroll J. J., Karamian S. A., Rivlin L. A., Zadernovsky A. A. // *Hyperfine Interact.* 2001. V. 135. P. 3.
2. Thomas K. E. // *Radiochim. Acta.* 1983. V. 34. P. 135;
Wilhelmy J. B. et al. // *Proc. 4th Intern. Conf. on Nuclei Far from Stability.* CERN, Geneva, 1981. P. 684.
3. Taylor W. A., Garcia J. G., Hamilton V. T. et al. // *J. Radioanal. Nucl. Chem.* 1998. V. 236. P. 155.
4. Kutschera W. et al. // *Proc. Intern. Conf. on Radioactive Nuclear Beams.* Singapore: World Scientific, 1990. P. 345.
5. Karamian S. A., Adam J., Filosofov D. V. et al. // *Nucl. Instr. Meth. A.* 2002. V. 489. P. 448.
6. Karamian S. A., Adam J., Chaloun P. et al. // *Nucl. Instr. Meth. A.* 2004. V. 527. P. 609.
7. Karamian S. A., Ur C. A., Adam J. et al. // *Nucl. Instr. Meth. A.* 2009. V. 600. P. 488.
8. Oganessian Yu. Ts., Karamian S. A., Gangrsky Yu. P. et al. // *J. Phys. G.* 1992. V. 18. P. 393.

9. *Oganessian Yu. Ts., Karamian S. A., Gangrsky Yu. P. et al. // Proc. Intern. Symp. on Nuclear Physics of Our Times. Singapore: World Scientific, 1993. P. 521.*
10. *Kim J. B., Trubert D., Constantinescu O. et al. // J. Radioanal. Nucl. Chem. 1997. V. 215. P. 219.*
11. *Karamian S. A. // Acta Phys. Polon. B. 1995. V. 26, No. 2–3. P. 375.*
12. *Baglin C.V. // Nucl. Data Sheets. 2009. V. 110. P. 265;*
Achterberg E., Capurro O.A. Marti G. // Nucl. Data Sheets. 2009. V. 110. P. 1473;
Kondev F. // Nucl. Data Sheets. 2003. V. 98. P. 801;
Basunia M.S. // Nucl. Data Sheets. 2006. V. 107. P. 791;
Basunia M.S. // Nucl. Data Sheets. 2004. V. 102. P. 719.
13. *Sikkeland T. // Arkiv för Fysik (Stockholm). 1967. V. 36. P. 539.*
14. *Jackson J. D. // Can. J. Phys. 1956. V. 34. P. 767.*
15. *Karamian S. A. JINR Preprint P4-11339. Dubna, 1978.*
16. *Bass R. // Nucl. Phys. A. 1974. V. 231. P. 45.*
17. *Volkov V. V. // Part. Nucl. 1975. V. 6. P. 1040.*
18. *Winther A. // Nucl. Phys. A. 1995. V. 594. P. 203.*
19. *Pollarolo G. // Phys. Rev. Lett. 2008. V. 100. P. 252701.*
20. *Baskova K. A. et al. // Izv. AN SSSR, Ser. Fiz. 1984. V. 48. P. 38.*
21. *Tulinov A. F. et al. // Izv. RAN, Ser. Fiz. 1993. V. 57. P. 135.*
22. *Chuvilskaya T. V., Shirokova A. A. // Izv. RAN, Ser. Fiz. 2008. V. 72. P. 1652.*
23. *Denisov V. Yu., Zheltonozhskii V. A., Reshit'ko S. V. // Phys. At. Nuclei (Yadernaya Fizika). 1993. V. 56. P. 57.*
24. *Oganessian Yu. Ts., Karamian S. A. // Hyperfine Interact. 1997. V. 107. P. 43.*
25. *Gorski B., Karamian S. A., Oganessian Yu. Ts. et al. // J. Radioanal. Nucl. Chem. 1993. V. 170. P. 353.*
26. *Dracoulis G. D. // Nucl. Instr. Meth. A. 1996. V. 382. P. 1;*
Walker P., Dracoulis G. // Nature. 1999. V. 399. P. 35.
27. *Ishii T., Sigematsu S., Asai M. et al. // Phys. Rev. C. 2005. V. 72. P. 021301(R).*
28. *Karamian S. A. // Phys. Atomic Nuclei. 2005. V. 68. P. 1827.*
29. *Karamian S. A., Carroll J. J., Adam J. et al. // High Energy Density Phys. 2006. V. 2. P. 48.*

Received on January 14, 2011.

Корректор *Т. Е. Попеко*

Подписано в печать 18.03.2011.

Формат 60 × 90/16. Бумага офсетная. Печать офсетная.

Усл. печ. л. 1,43. Уч.-изд. л. 1,93. Тираж 260 экз. Заказ № 57275.

Издательский отдел Объединенного института ядерных исследований
141980, г. Дубна, Московская обл., ул. Жолио-Кюри, 6.

E-mail: publish@jinr.ru

www.jinr.ru/publish/